Cellular Signalling 61 (2019) 66–77

Contents lists available at ScienceDirect

Cellular Signalling

journal homepage: www.elsevier.com/locate/cellsig

Hydrogen sulphide mitigates homocysteine-induced apoptosis and matrix remodelling in mesangial cells through Akt/FOXO1 signalling cascade

Suravi Majumder[a], Lu Ren[b], Sathnur Pushpakumar[a], Utpal Sen[a,*]

[a] Department of Physiology, University of Louisville School of Medicine, Louisville, KY, United States of America
[b] Department of Pathology and Laboratory Medicine, Indiana University School of Medicine, Indianapolis, IN, United States of America

ARTICLE INFO

Keywords:
Homocysteine
Collagen
Fibronectin
MMP
Caspase
GYY4137

ABSTRACT

Cellular damage and accumulation of extracellular matrix (ECM) protein in the glomerulo-interstitial space are the signatures of chronic kidney disease (CKD). Hyperhomocysteinemia (HHcy), a high level of homocysteine (Hcy) is associated with CKD and further contributes to kidney damage. Despite a large number of studies, the signalling mechanism of Hcy-mediated cellular damage and ECM remodelling in kidney remains inconclusive. Hcy metabolizes to produce hydrogen sulphide (H_2S), and a number of studies have shown that H_2S mitigates the adverse effect of HHcy in a variety of diseases involving several signalling molecules, including forkhead box O (FOXO) protein. FOXO is a group of transcription factor that includes FOXO1, which plays important roles in cell growth and proliferation. On the other hand, a cell survival factor, Akt regulates FOXO under normal condition. However, the involvement of Akt/FOXO1 pathway in Hcy-induced mesangial cell damage remains elusive, and whether H_2S plays any protective roles has yet to be clearly defined. We treated mouse mesangial cells with or without H_2S donor, GYY4137 and FOXO1 inhibitor, AS1842856 in HHcy condition and determined the involvement of Akt/FOXO1 signalling cascades. Our results indicated that Hcy inactivated Akt and activated FOXO1 by dephosphorylating both the signalling molecules and induced FOXO1 nuclear translocation followed by activation of the FOXO1 transcription factor. These led to the induction of cellular apoptosis and synthesis of excessive ECM protein, in part, due to increased ROS production, loss of mitochondrial membrane potential ($\Delta\Psi m$), reduction in intracellular ATP concentration, increased MMP-2, -9, -14 mRNA and protein expression, and Col I, IV and fibronectin protein expression. Interestingly, GYY4137 or AS1842856 treatment prevented these changes by modulating Akt/FOXO1 axis in HHcy. We conclude that GYY4137 and/or AS1842856 mitigates HHcy induced mesangial cell damage and ECM remodelling by regulating Akt/FOXO1 pathway.

1. Introduction

Hyperhomocysteinemia (HHcy), an increased plasma homocysteine (Hcy) level is prevalent among patients with chronic kidney diseases (CKD) [1]. The mesangial cell provides architectural support for glomerular capillary loops and is a crucial player in the initiation and progression of many kidney diseases [2,3]. Increased glomerular mesangial cell apoptosis/proliferation and excessive accumulation of extracellular matrix (ECM) protein lead to glomerulosclerosis in CKD patients [4,5]; similar results are also reported in experimental CKD animals [6–8]. However, the precise cellular mechanisms of HHcy-induced progressive glomerular damage, sclerosis and dysfunction remain elusive.

PI3K/Akt/FOXO signalling pathway is an essential regulator of cell survival and apoptosis [9,10]. Akt, the serine/threonine kinase protein kinase B, was identified as a downstream component in survival signalling through phosphatidylinositol-3 kinase (PI3K). The Akt kinase is activated by phosphorylation at Thr308 and Ser473 mediated by 3-phosphoinositide-dependent protein kinase 1 and 2, respectively [11,12]. After phosphorylation at Thr308 and Ser473 position, activated Akt phosphorylates many substrates. The subgroup O of forkhead box (FOXO) transcription factors are major substrates for Akt. Akt phosphorylates FOXOs at three conserved serine/threonine residues (Thr24, Ser256, Ser319), facilitating their association with 14-3-3 chaperone and leading to nuclear export and transcriptional activation [13]. The FOXO family consists of four members, FOXO1, FOXO3, FOXO4 and FOXO6 that share a conserved forkhead DNA-binding domain [14]. FOXOs therefore have emerged as an important effector arm of PI3K/Akt signalling by driving multiple cellular processes such as apoptosis, cell cycle, oxidative stress, DNA damage repair and glucose

* Corresponding author at: University of Louisville School of Medicine, Louisville, KY 40202, United States of America.
E-mail address: u0sen001@louisville.edu (U. Sen).

https://doi.org/10.1016/j.cellsig.2019.05.003
Received 18 December 2018; Received in revised form 28 March 2019; Accepted 2 May 2019
Available online 11 May 2019
0898-6568/

metabolism [15]. Recent reports illustrated that FOXO1 plays critical roles in the cell cycle, proliferation, apoptosis, and tumorigenesis by regulating the expression of its target genes [16]. Based on these previous reports, we hypothesize that FOXO1 may play a direct role in Hcy-induced mesangial cell apoptosis and ECM remodelling.

Hcy-induced cell apoptosis has been studied in various cell types including neuronal [17], promyeloid [18], endothelial [19,20], and mesangial cells [21]. The study in mesangial cells showed that Hcy induces apoptosis by activating p38-mitogen-activated protein kinase [21]. Hcy was also shown to induce cell cycle arrest through PI3K/Akt/FOXO pathway in endothelial cells [22]. Our laboratory has previously reported that Hcy-induced apoptosis was mediated through generation of ROS that played a major role in ECM remodelling in HHcy-associated CKD [7]. Along the same line, our laboratory had previously demonstrated mesangial cell death and ECM expansion that were directly linked to glomerulosclerosis [11,12], and H_2S supplementation mitigated ECM remodelling [23,24]. GYY4137, a H_2S donor is now well-established compound that protects renal and cardiovascular fibrosis [25,26]. The molecular signalling mechanism of these protections, however, has yet to be completely defined.

In the present study, we aimed at delineating the role of the Akt/FOXO signalling pathway in Hcy-mediated mesangial cell apoptosis and ECM accumulation. We also investigated whether and how H_2S donor, GYY4137 modulates Akt/FOXO1 signalling pathway to mitigate Hcy-induced mesangial cell death and ECM remodelling.

2. Materials and methods

2.1. Antibodies and reagents

Primary antibodies against phospho-Akt (Cell Signalling, 9271); total Akt (44-609G), phospho-FOXO1 (PA5–37577), total FOXO1 (MA5–17078), MMP-2 (PA1–16667); MMP-9 (MA5–15886) were from Thermo Fisher Scientific (Waltham, MA). MMP-14 (ab53712), Fibronectin (ab2413), ATP assay kit (ab83355), and FOXO1 transcription factor assay kit (ab207204) were purchased from Abcam (Cambridge, UK). Collagen-I (NBP1–30054) and Collagen-IV (NBP1–26549) were from Novus Biologicals (Centennial, CO). Cleaved caspase-3 (mAb9664) and cleaved caspase-7 (mAb8438) were from Cell Signalling (Danvers, MA). The β-actin (sc81178), and HRP conjugated secondary antibodies that we used for immune-detection were from Santa Cruz Biotechnology (Dallas, TX). GYY4137 and L-Homocysteine, *N*-acetyl cysteine (NAC) was from Sigma-Aldrich, St. Louis, MO; and AS1842856 was from EMD Millipore, Burlington, MA. MK2206 was from Selleckchem, Houston, TX; PVDF membrane was from Bio-Rad (Hercules, CA) and dihydroethidium (DHE) was from Invitrogen (Carlsbad, CA). JC-1 dye and Caspase3/7 green detection reagents were purchased from Thermo Fisher Scientific, Waltham, MA. Tunnel, and all other analytical reagents were from Sigma-Aldrich (St. Louis, MO) or available highest grade. Epiquik nuclear extraction kit (OP-0002-1), Direct-zol RNA miniprep (R2050S) were from Epigentek (Farmingdale, NY). EasyScript cDNA synthesis kit (G234) was from Midsci (Valley Park, MO), and GoTaq Hot start green mastermix (M512B) was from Promega (Madison, WI).

2.2. Cell cultures and treatments

Mouse SV40 MES 13 (murine mesangial) cells were obtained from the American Type Culture Collection (Rockville, MD). Cells were cultured and maintained in a complete DMEM/F12 medium (3:1) at 37 °C with 5% CO_2, and were seeded onto 6-well culture plates at an equal density. At 80% confluence, cells were treated with Hcy (50 μM), GYY4137 (250 μM) and AS1842856 (0.1 μM) alone or with a combination. Inhibitors were added 1 h prior to Hcy treatment. Cells were treated for 30 min for activation assay and 24 h for all other experiments.

2.3. Assessment of cell apoptosis

2.3.1. AnnexinV/PI assay

An Annexin V-FITC early apoptosis detection kit (Cell Signalling Technology, Inc.; Danvers, MA) was used to identify the apoptotic cells within a cell population. Briefly, the cells were treated for 24 h and then trypsinized and collected by centrifugation, washed thrice with ice-cold PBS and re-suspended at 10^5 cells/ml with 1× Annexin V Binding Buffer. Then, 1 μl of Annexin V-FITC conjugate and 12.5 μl of Propidium Iodide (PI) solution were added to each cell suspension (96 μl) and incubated 15 min on ice in the dark. Next, the cell suspension was diluted to a final volume of 250 μl/assay with ice-cold 1× Annexin V Binding Buffer and analyzed immediately using a FACS (Accuri C6 plus Flow Cytometer, BD Bioscience).

2.3.2. TUNEL assay

The terminal deoxynucleotidyltransferase-mediated dUTP-biotin nick end labelling (TUNEL) assay was performed to detect mesangial cell apoptosis using in situ cell death detection kit, Fluorescein following the manufacturer's instructions (Roche, Sigma Aldrich). Mesangial cells were seeded onto a chambered slide, and maintained in complete DMEM and treated with Hcy with or without GYY4137 and AS1842856 for 24 h. Cells were fixed with fixation solution for 20 min at room temperature, washed twice with PBS, then permeabilized with permeabilization solution for 5 min on ice. Cells were then washed twice with PBS. Fixed cells were incubated with 50 μl TUNEL reaction mixture for 60 min at room temperature, washed twice with PBS, and fluorescence microscopic analyses were performed.

2.4. Detection of reactive oxygen species (ROS)

ROS was detected in mesangial cells using the Dihydroethidium (DHE) staining method as described previously [7]. Briefly, cells were fixed in 4% paraformaldehyde for 10 min, air-dried and then washed with ice-cold PBS. Cells were then incubated with DHE (0.5 μM) in a dark humidified chamber for 10 min at 37 °C. Cells were washed twice with PBS and were mounted with FluoroGel mounting medium (GeneTex Inc., Irvine, CA). Images were taken by a laser scanning confocal microscope (Olympus FluoView 1000, Pittsburgh, PA) and analyzed using ImageJ software (NIH).

2.5. Assessment of mitochondrial membrane potential (ΔΨm)

To assess the loss of ΔΨm, fluoroprobe 5,5′,6,6′-tetrachloro-1,1′,3,3′-tetraethylbenzimidazol-carbocyanine iodide (JC-1 dye) was used. Briefly, cells were exposed to Hcy with or without GYY4137 and AS1842856 for 24 h. After treatment, cells were washed with PBS followed by staining with 2 μg/ml of JC-1 dye for 15 min in dark at 37 °C. Cells were then washed thoroughly with PBS and imaged in a confocal microscope (Olympus FluoView1000, Pittsburgh, PA). At a lower ΔΨm, JC-1 exists as a monomer and is visible in the green fluorescence channel. At a higher ΔΨm, JC-1 accumulates in the mitochondrial matrix and is visible in the red channel. Therefore, a decrease in ΔΨm could be detected by the transition from red to green fluorescence.

2.6. ATP concentration measurement

The ATP levels were measured using an ATP Colorimetric/Fluorometric Assay Kit (Abcam 83355), according to the manufacturer's instructions. The absorbance was recorded by spectrophotometer at OD 570 nm.

2.7. Detection of caspase 3/7 activity

After treatment, cells were labeled with 5 μM CellEvent™ caspase-3/7 green detection reagent in complete medium for 30 min at 37 °C in the

Table 1
Primers sequence, melting temperature (Tm), and accession number/reference. F, forward; R, reverse.

Primers	Sequence	Tm (°C)	Accession number/Reference
MMP-2	F: 5′CACCTACACCAAGAACTTCCGA3′ R: 5′ACCAGTGTCAGTATCAGCATCG3′	57.1	NM_008610
MMP-9	F: 5′CACACGACATCTTCCAGTACCA3′ R: 5′TCATTTTGGAAACTCACACGCC3′	57	NM_013599
MMP-14	F: 5′GGATGGACACAGAGAACTTCGT3′ R: 5′GTGACCCTGACTTGCTTCCATA3′	57	NM_008608
GAPDH	F: 5′GTCGTGGAGTCTACTGGTGT3′ R: 5′TGCTGACAATCTTGAGTGAG3′	53.1	[60]

dark. Stained cells were washed twice with PBS, mounted with DAPI mounting medium, and observed under a fluorescence microscope. Apoptotic cells with activated caspase-3/7 show bright green nuclei, while cells without activated caspase-3/7 exhibit minimal fluorescence signal.

2.8. RNA extraction and semi-quantitative reverse transcription-PCR (RT-PCR)

RNA was extracted from cells by using the Direct-zol RNA miniprep kit. The quality of total RNA was measured by NanoDrop ND-1000 and only high-quality RNA (260/280–2.00 and 260/230–1.80) was used for reverse transcriptase PCR. The total RNA (2 μg) was reverse transcribed by using the Easyscript cDNA synthesis kit according to the manufacturer's instructions. PCR program for amplification of cDNA was performed using GoTaq Hot start green Master Mix (Promega) according to manufacturer's guidelines. The primer sequences and their accession/reference numbers are listed in Table 1.

2.9. Western blot analysis

Protein was extracted from cells using RIPA buffer (Boston BioProducts, Worcester, MA), containing 1 mM phenylmethanesulfonyl fluoride (PMSF), and 1% protease inhibitor cocktail (Sigma-Aldrich, Saint Louis, MO). After sonication, protein lysate was centrifuged at 12,000 × *g* for 10 min at 4 °C. Protein concentration was measured by Bradford assay. An equal amount of protein extract (25 μg) was electrophoretically separated by SDS-PAGE and immunoblotted onto PVDF membrane. The membranes were blocked with 5% non-fat milk for 60 min at room temperature and subsequently incubated with respective primary antibodies for overnight at 4 °C. Membranes were washed three times with PBS followed by 2 h incubation with respective secondary antibodies at room temperature. The membranes were washed to remove unbound secondary antibodies, and protein bands were visualized using ECL Luminata Forte (Millipore, Temecula, CA) in a Bio-Rad ChemiDoc system. Band intensity was quantified using ImageJ software.

2.10. Immunofluorescence

Cells were fixed in 4% paraformaldehyde for 10 min and washed thrice with ice-cold PBS. Cells were then permeabilized with 0.25% Tween 20 in PBS for 10 min and washed thrice with PBST (0.1% Tween 20). Cells were incubated in blocking buffer (1% BSA in PBST) for 1 h, washed and then primary antibody (1:1000) was added and incubated at 4 °C for overnight with gentle shaking. Secondary antibodies labeled with Alexa Fluor (Invitrogen) appropriate to the primary antibody species were applied to the cells for immunodetection. After washing with PBST cells were immediately visualized under a laser scanning confocal microscope (Olympus FluoView1000, Pittsburgh, PA) and images were captured using appropriate filters. Images were further analyzed for fluorescence intensity using ImageJ software.

2.11. FOXO1 transcription factor activity assay

Cell nuclear extracts were obtained from mesangial cells by using the Epiquik nuclear extraction kit (OP-0002-1). FOXO1 transcription factor activity assay was performed by using an ELISA kit (ab207204) according to manufacturers' instruction. The absorbance was recorded by spectrophotometer at OD 450 nm.

2.12. Statistical analysis

ImageJ software was used to calculate the mean values of protein expression. Data were expressed as mean ± SEM, $n = 8–9$ independent experiments as stated in the figure legends. The significant difference was determined by one-way ANOVA within and across different effectors or inhibitors for repeated measures using GraphPad Prism. The significance was accepted at the level of $p < .05$.

3. Results

3.1. Hcy-induced Akt/FOXO1 signalling was prevented by GYY and AS

Hcy treatment decreased phosphorylation of Akt and FOXO1 in mesangial cells as measured by Western blot (Fig. 1A, B). Hcy treatment deactivated Akt by inhibiting phosphorylation of Akt, which in turn dephosphorylated FOXO1. After dephosphorylation, FOXO1 becomes transcriptionally active and translocates into the nucleus to activate its target genes [13]. The results of our study showed that Hcy-induced activation of FOXO1 was reversed by GYY treatment. A selective inhibitor FOXO1, AS which blocks transcription activity of FOXO1 [27], also suppressed Hcy-induced dephosphorylation and activation of FOXO1 in mesangial cells. We also measured whether Hcy induced nuclear translocation of FOXO1 because of its activation. Our results indicated that phosphorylated FOXO1/total FOXO1 (pFOXO1/tFOXO1) ratio in Hcy treated cells was significantly lower in nuclear fraction and higher in cytosolic fraction compared to their respective controls (Fig. 1C, D). These results indicated the nuclear translocation of FOXO1 following Hcy-induced FOXO1 activation. Interestingly, GYY or AS treatment prevented the nuclear translocation of FOXO1 in Hcy-treated cells (Fig. 1C, D). No significant changes in terms of FOXO1 nuclear translocation were measured in cells treated with either GYY or AS alone (Fig. 1C, D). Additionally, we also measured FOXO1 activity following Hcy treatment with or without GYY, or AS. Corroborating with the immunoblotting results, activity assay demonstrated upregulated FOXO1 activity following Hcy treatment, which was mitigated and normalized by GYY or AS treatment (Fig. 1E). No significant changes were observed in cells treated with GYY or AS alone compared to control (Fig. 1E).

3.2. GYY and AS mitigated Hcy-induced MMPs induction and ECM protein expression

MMPs are involved in ECM degradation, and therefore cause tissue remodelling in various physiological conditions [7,28]. Hcy stimulates MMPs, in part, by oxidative activation and thus contributes to tissue remodelling [7]. On the contrary, Hcy also oxidatively modifies ECM proteins that MMPs cannot degrade and therefore causes fibrosis [29]. Our results indicated that Hcy increased MMP-2, -9, and -14 mRNA (Fig. 2A) and protein (Fig. 2B) expression in mesangial cells compared to control cells, which were normalized by GYY treatment. Furthermore, Hcy induced increased MMP -2, -9, -14 mRNA and protein expression was also normalized by FOXO1 inhibitor AS, suggesting the involvement of FOXO1 signalling in regulating these above MMPs, both at the mRNA and the protein levels. In drug control cells, i.e. in cells that were treated with GYY or AS alone, none of these above three

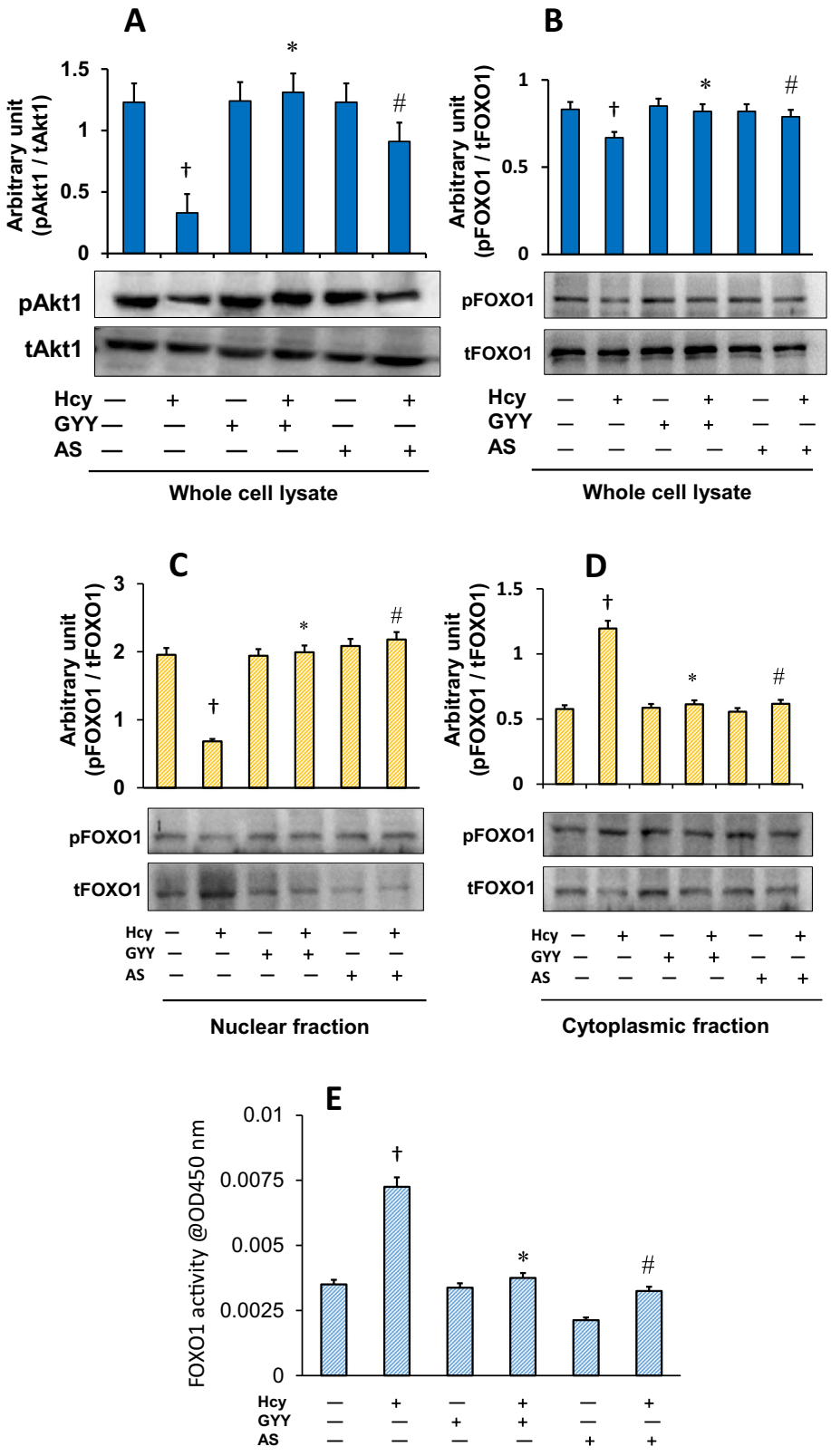

Fig. 1. A,B GYY4137 (GYY) and AS1842856 (AS) inhibited Hcy-induced Akt and FOXO1 signalling in mesangial cells. A) Hcy (50 μM, 30 min) deactivated Akt by dephosphorylation, and B) activated FOXO1 by dephosphorylation in mesangial cells as measured by Western blotting in whole cell lysates. GYY and AS inhibited the effect of Hcy. Bar graphs represent ratio of phospho-Akt to total-Akt (pAkt/tAkt (A) and phospho-FOXO1 to total-FOXO1 (pFOXO1/tFOXO1) (B). Data represents mean ± SEM, $n = 9$ independent experiments; $^{\dagger}p < .05$ vs Control (no treatment); $^{*,\#}p < .05$ vs Hcy alone treatment.
(C, D) Hcy-induced nuclear translocation of FOXO1 was blocked by GYY4137 (GYY) and AS1842856 (AS). C) Nuclear extract of mesangial cells treated with Hcy showed a higher expression of total-FOXO1 in compared to other groups (C), whereas cytosolic extract showed reduced total-FOXO1 expression (D) indicating nuclear translocation of FOXO1 by Hcy. This indicates Hcy-induced FOXO1 transcription factor activation in mesangial cells. GYY and AS have shown to prevent the FOXO1 nuclear translocation and activation. In the bar graphs, data represents mean ± SEM, $n = 9$ independent experiments; $^{\dagger}p < .05$ vs control (no treatment), $^{*,\#}p < .05$ vs Hcy alone treatment.
(E) Hcy-induced increased FOXO1 activity was normalized by GYY4137 (GYY) or AS1842856 (AS) treatment. The mesangial cells were grown in 6-well culture plates and treated with Hcy, GYY and/or AS for 24 h. FOXO1 activity levels in the nuclear extracts were measured by ELISA based colorimetric kit (ab207204). The bar diagram represents relative FOXO1 activity; data mean ± SEM, $n = 9$ independent experiments; $^{\dagger}p < .05$ vs control (no treatment), $^{*,\#}p < .05$ vs Hcy alone treatment.

MMPs gene or protein expression was significantly changed compared to negative controls (Fig. 2A,B).

We also investigated the effect of GYY on Hcy-induced altered expression of ECM proteins Collagen I (Col I), Collagen IV (Col IV) and fibronectin (Fbn-1) and the results are shown in Fig. 3. Hcy induced the expression of Col I, Col IV and Fbn-1 in mesangial cells as measured by Western blotting. Interestingly, GYY or AS treatment mitigated the expression of these proteins in HHcy (Fig. 3). GYY or AS alone had no effect in the expression of these above ECM proteins in control cells, i.e., without Hcy treatment (Fig. 3).

Further studies with immunofluorescence labelling confirmed that Hcy induced increased expression of MMP-14 and Col IV (Fig. 4A) and

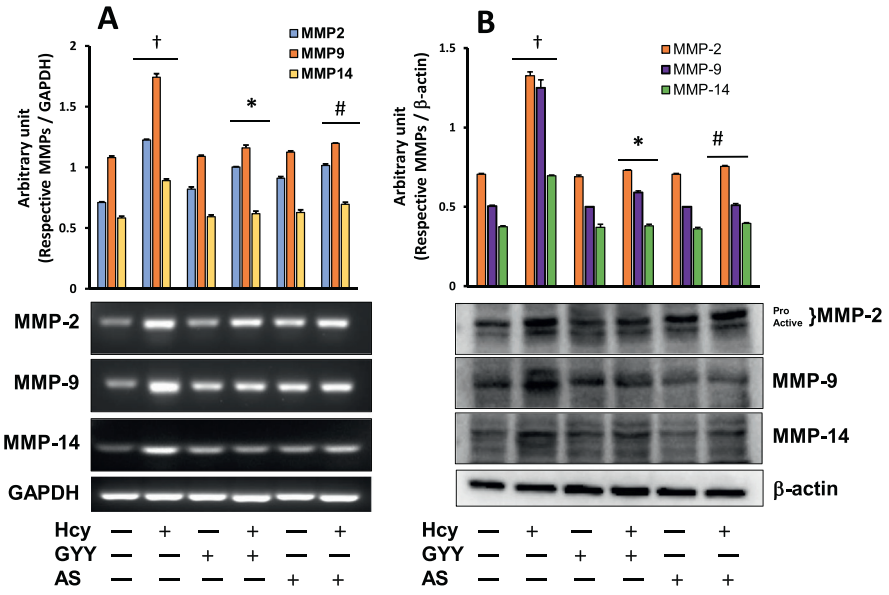

Fig. 2. Hcy-induced overexpression of MMP-2, -9 and -14 mRNA (A) and protein (B) was normalized in mesangial cells following GYY4137 (GYY) and AS1842856 (AS) treatment. The mRNA expression was measured by RT-PCR (A), and immunoblots represent protein expression as measured by Western blotting (B). Bar graphs represent densitometric analyses of mRNA and protein expression normalized with GAPDH and ß-actin, respectively. Values are mean ± SEM, $n = 9$ independent experiments. $^{\dagger}p < .05$ vs. no treatment (control) and $^{*,\#}p < .05$ vs. Hcy alone treatment.

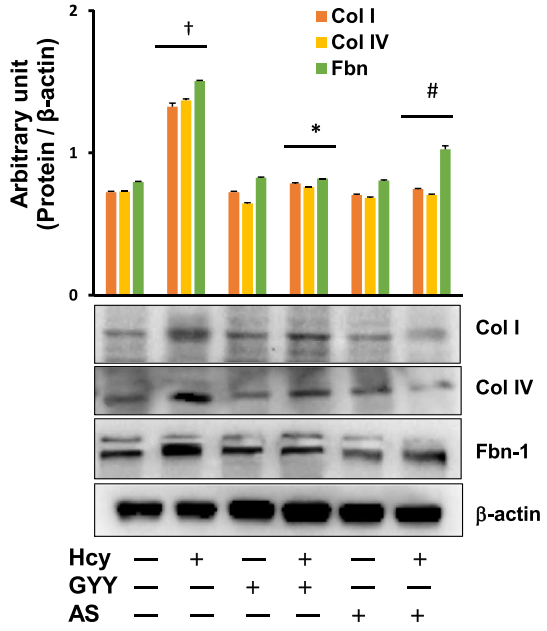

Fig. 3. Hcy-induced altered expression of collagen I, IV (Col I, Col IV) and Fibronectin (Fbn) was normalized in mesangial cells following GYY4137 (GYY) and AS1842856 (AS) treatment. Protein expression of Col I, Col IV and Fbn in mesangial cells was measured by Western blotting (immunoblots). The bar graph represents densitometric analyses of Col I, Col IV and Fbn protein expression normalized with ß-actin. Values are mean ± SEM, $n = 9$ independent experiments; $^{\dagger}p < .05$ vs. no treatments (Control) and $^{*,\#}p < .05$ vs. Hcy treatment.

Fbn-1 (Fig. 4B) in mesangial cells was also attenuated by GYY or AS.

3.3. Hcy-induced apoptosis was mitigated by GYY and AS via Akt/FOXO1 pathway

We determined Hcy-induced mesangial cell apoptosis by Annexin V/PI staining and TUNEL assay. Flow cytometry assay indicated that Hcy significantly increased apoptotic cell death compared to control (Fig. 5A, B). This increase was attenuated by GYY treatment. To determine whether Akt/FOXO1 signalling pathway was involved in Hcy-induced cell death, we treated mesangial cells with Akt inhibitor, MK2206 (MK) and FOXO1 inhibitor, AS1842856 (AS). Our results indicated that blocking of FOXO1 by AS diminished Hcy-mediated cell apoptosis, whereas Akt inhibition by MK2206 triggered Hcy-induced cell death (Fig. 5A, B). These flow cytometry findings were further supported by similar experiments with TUNEL staining (Fig. 5C); whereas GYY, MK or AS alone did not have an effect on cell apoptosis as measured by flow cytometry or TUNEL assay. Together, these results suggest that Hcy inhibits Akt and activates FOXO1 to promote mesangial cell apoptosis, which can be attenuated by H_2S treatment (Fig. 5A–C).

3.4. GYY and AS prevented Hcy-induced Caspase-3/7 activation

Loss of ΔΨm triggers caspase activation, which is a characteristic and stereotyped feature of cell undergoing apoptosis. Further investigation of Hcy-induced mesangial cell apoptosis, as we have measured in our experiments reported in Fig. 5A–C, we performed caspase-3/7 activity assay in experimental and control cells. Results showed that mesangial cells treated with Hcy manifested increased caspase-3/7 activity compared to control (Fig. 6A). Interestingly, this increased activity was prevented either by GYY or AS treatment along with Hcy. GYY or AS lone did not affect caspase-3/7 basal activity (Fig. 6A). Further analyses of caspases-3/7 by Western blotting indicated the upregulation of cleaved caspases-3/7 expression by Hcy in mesangial cells, which were normalized by GYY or AS treatment (Fig. 6B). Similar to immunostaining results neither GYY nor AS alone affected cleaved caspase-3/7 expression in these cells. These results further support our observation of Hcy-induced apoptosis (Fig. 5), and indicate that the apoptosis is in part by activation of caspase-3/7 (Fig. 6A,B).

3.5. GYY and AS mitigated Hcy-induced ROS production

ROS production in mesangial cells was measured using oxidative fluorescent dye DHE, where red fluorescence indicates ROS production. Hcy robustly and significantly increased ROS production in mesangial cells compared to control cells (Fig. 7A,B). Interestingly, GYY or AS treatment significantly diminished DHE fluorescence indicating prevention of ROS production in Hcy treated cells. No apparent change in basal ROS production was observed in GYY or AS alone treated cells (Fig. 7A,B).

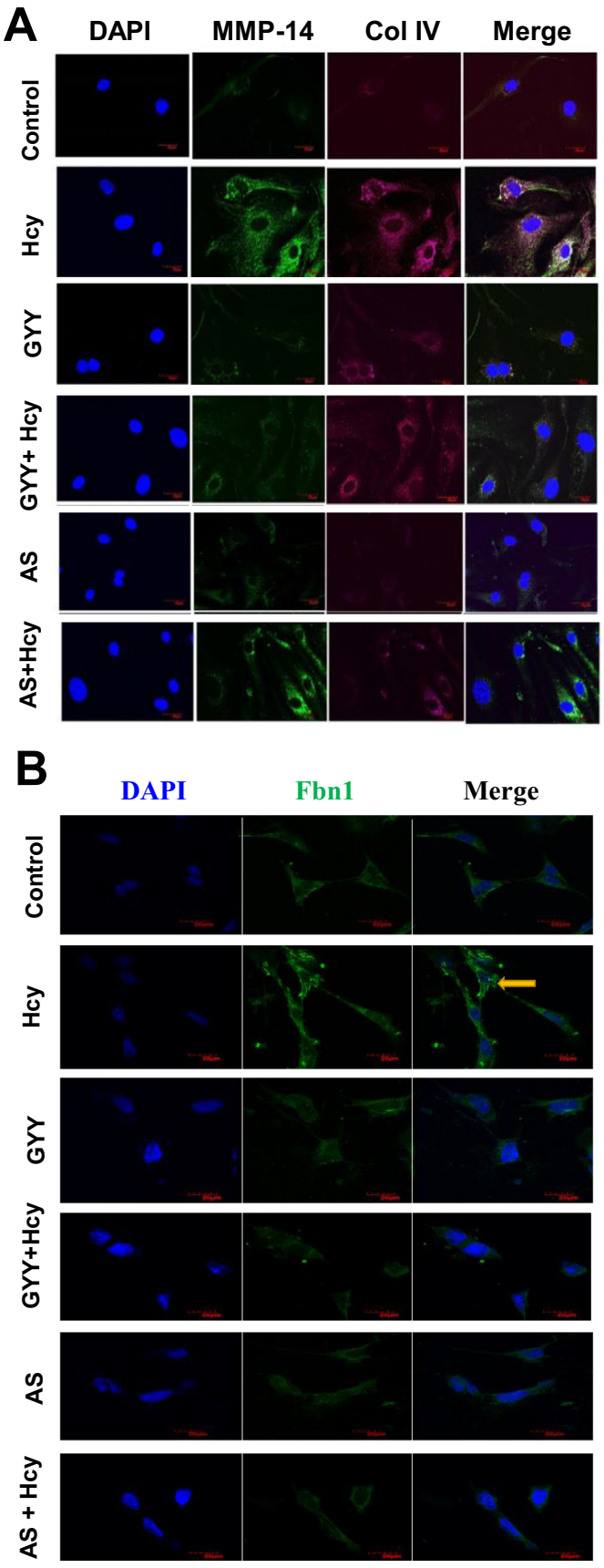

Fig 4. (A) Hcy-induced increased expression and localization of MMP-14 and Collagen IV (Col IV) in mesangial cells was mitigated by GYY4137and AS1842856. Control and treated cells were incubated with primary antibodies and counterstained with appropriate secondary antibodies. Immunofluorescence images of the cells expressing MMP-14 (green) and Col IV (red) were captured under a fluorescence microscope. Representative images are from $n = 8$ independent experiments. Original magnification 100×; Scale bar: 20 μm. (For interpretation of the references to colour in this figure legend, the reader is referred to the web version of this article.)
(B) Hcy-induced expression of Fbn1 in mesangial cells was mitigated by GYY4137 (GYY) and AS1842856 (AS). Control and treated cells were incubated with primary Fbn1 antibody and counterstained with appropriate secondary antibody. Immunofluorescence images of the cells expressing Fbn1 were captured under a fluorescence microscope. Representative images are from $n = 8$ independent experiments. Original magnification 100×; Scale bar: 20 μm.

3.6. Inhibition of ROS by NAC mitigated Hcy-induced MMPs and matrix protein induction

To determine whether Hcy-induced ROS induces MMPs and ECM proteins, we pre-treated mesangial cells with *N*-acetyl cysteine (NAC) and then treated with Hcy. Results indicated that Hcy increased MMP-2, -9, and -14 protein expression in cells, which were normalized by NAC pre-treatment (Fig. 8A). The expression of these MMPs was at the baseline levels and remained unchanged in control groups with or without NAC. Similar to MMPs expression, matrix protein Col 1, Col IV and Fbn were upregulated in Hcy treated groups (Fig. 8B). Interestingly, the upregulation of these matrix proteins were mitigated by NAC treatment. Virtually no differences were observed in immunoblots in the control groups treated with or without NAC (Fig. 8B).

3.7. GYY and AS mitigated Hcy-induced mitochondrial dysfunction

Excess ROS generation can lead to mitochondrial dysfunction resulting in lower mitochondrial membrane potential (ΔΨm). Loss of ΔΨm is an important factor for the induction of cell apoptosis [27]. We measured the change of ΔΨm in mesangial cells exposed to Hcy. Our results indicated that Hcy treatment significantly decreased the red signal intensity while increasing the green signal intensity compared to control, which is indicative of collapsed ΔΨm (Fig. 9A,B). On the other hand, GYY treatment preserved increased red signal and decreased green signal intensity in Hcy treated cells indicating a normalization of ΔΨm. A similar result was observed following AS treatment in Hcy treated cells (Fig. 9A,B). Although a non-significant change in red/green colour ratio in GYY treated control cells was observed, in AS alone treated cells a significant reduction of ΔΨm, as measured by red/green ratio, was observed compared to control. However, this change was comparable to GYY alone (Fig. 9A,B). To further determine whether Hcy-induced loss of Δψm has any effect on intracellular ATP production in mesangial cells, we measured intracellular ATP concentration by using an assay kit as described in the materials and methods. Our result indicated that Hcy decreased intracellular ATP concentration by about 50% in mesangial cells (Fig. 9C). This decreased intracellular ATP concentration was restored by GYY or AS treatment in Hcy treated cells. No effects of GYY or AS alone on intracellular ATP concentration was observed (Fig. 9C). These results suggest that GYY and/or AS prevents Hcy-induced mitochondrial dysfunction by preserving ΔΨm and intracellular ATP concentration.

4. Discussion

Hyperhomocysteinemia (HHcy) is associated with chronic kidney disease (CKD) and increased plasma Hcy levels are linked to renal fibrosis [30–32]. Excessive accumulation of extracellular matrix (ECM) protein and upregulation of matrix metalloproteinases (MMPs) are major contributing factors leading to Hcy-mediated renal fibrosis and

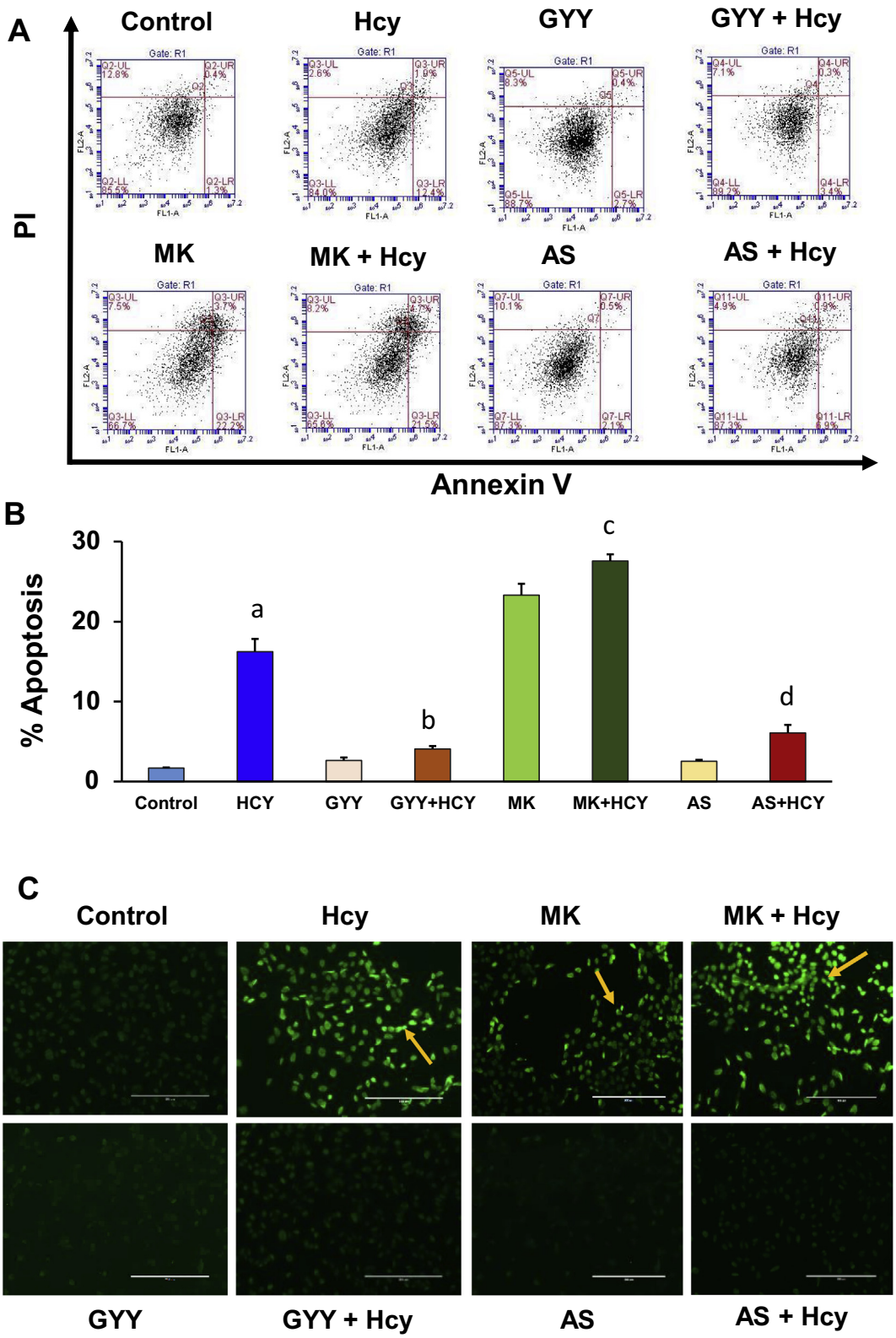

Fig. 5. (A, B) GYY4137 (GYY) and AS1842856 (AS) mitigated apoptotic cell death in high Hcy treated mesangial cells. (A) Flow cytometric analysis of cell death by using Annexin V-FITC/PI staining of apoptotic cells (early & late apoptosis). Mesangial cells were treated with Hcy (50 μM, 24 h) in combination with or without GYY and AS. The viable cell populations are in the lower left quadrant (Annexin V-/PI-). The cells at the early apoptosis are in the lower right quadrant (Annexin V + /PI-), and the ones at the late apoptosis are in the upper right quadrant (Annexin V + /PI +). (B) Percent of apoptotic cells were shown in this bar diagram. Values are mean ± SEM, $n = 8$ independent experiments; $^{a}p < .05$ versus control; $^{b,c,d}p < .05$ versus Hcy treated cells. MK (MK2206), an Akt inhibitor.
(C) Fluorescence microscopic imaging of mesangial cells stained by TUNEL reagent to detect apoptotic cells. Bright green cells are apoptotic positive cells (20×). Arrows indicating TUNEL positive cells. Representative images are from $n = 8$ independent experiments. MK (MK2206), an Akt inhibitor. (For interpretation of the references to colour in this figure legend, the reader is referred to the web version of this article.)

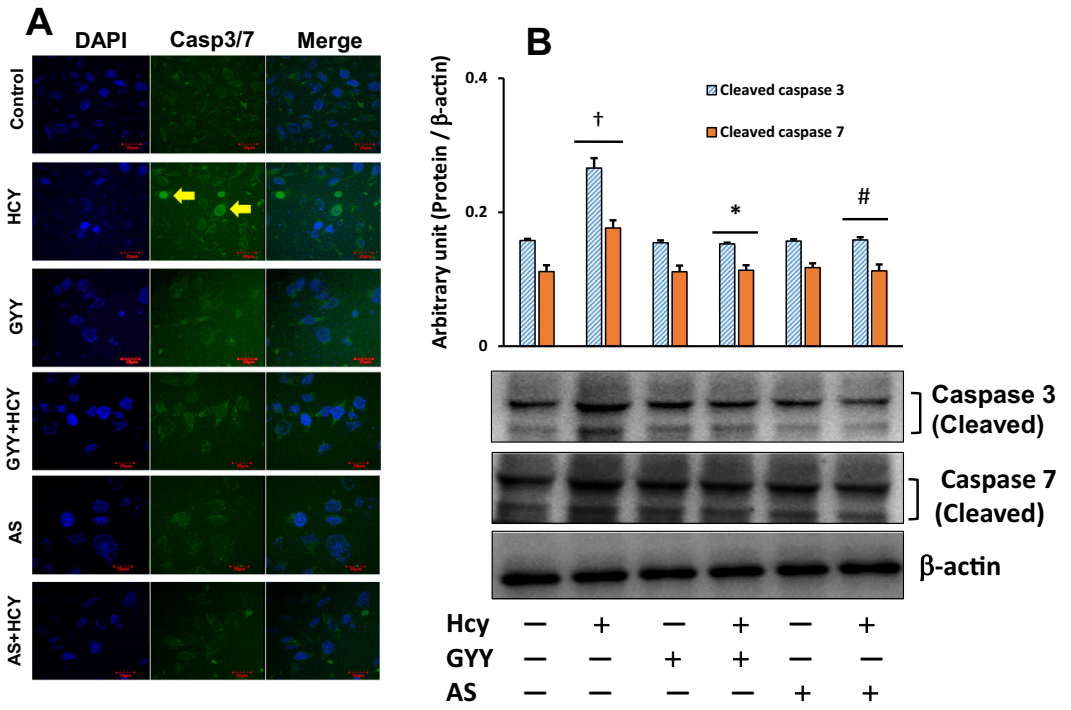

Fig. 6. (A, B) GYY4137 (GYY) and AS1842856 (AS) mitigated caspase-3/7 expression in Hey treated cells. (A) Fluorescence images showing Hcy induced caspase-3/7 in mesangial cells. Following Hcy, GYY and AS treatments, cells were stained with CellEvent Caspase-3/7 Green reagent for 15 min. Nucleus was stained with DAPI. Scale bar is 20 μm. Caspase-3/7 positive cells exhibited bright green fluorescence; whereas, cells negative to caspase-3/7 exhibited no fluorescence. Arrows are indicating Caspase-3/7 positive cells. Representative images are from $n = 8$ independent experiments. (B) Hcy-induced increased expression of caspase-3/7, as measured by Western blotting, was mitigated by GYY and AS treatment. The bar graph represents densitometric analyses of cleaved caspase-3/7 protein expression, which was normalized with ß-actin. Values are mean ± SEM, $n = 9$ independent experiments; $^{\dagger}p < .05$ vs. no treatments (control) and $^{*,\#}p < .05$ vs. Hcy treatment. (For interpretation of the references to colour in this figure legend, the reader is referred to the web version of this article.)

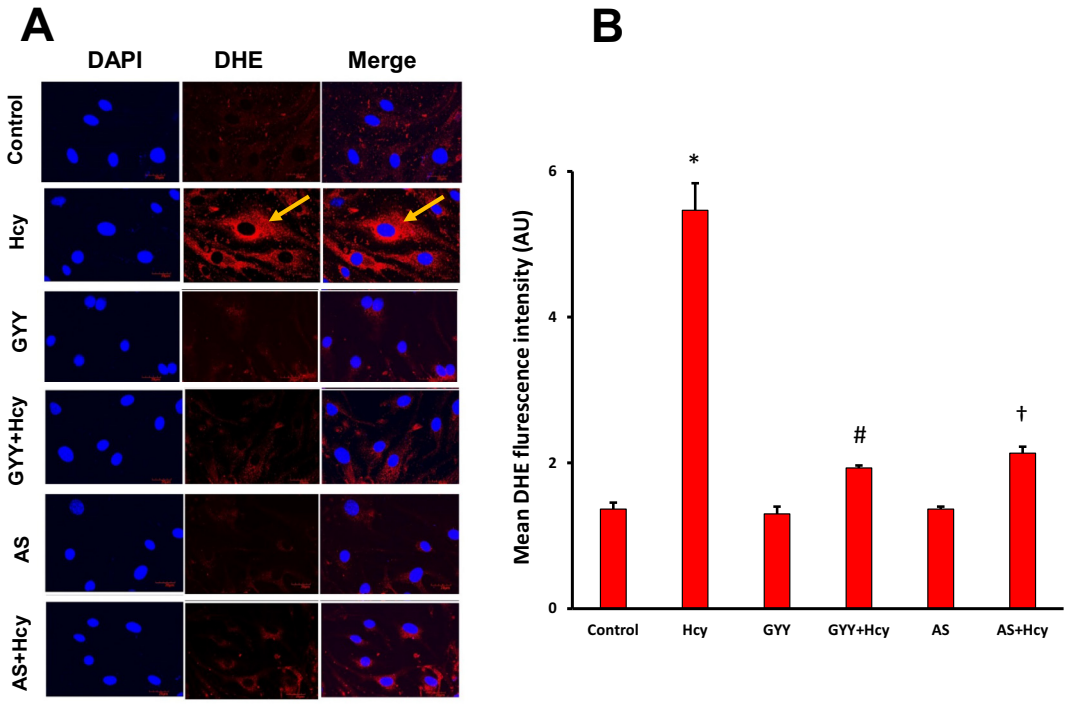

Fig. 7. Increased ROS by Hcy was diminished by either GYY4137 (GYY) or FOXO1 inhibitor, AS1842856 (AS) treatment in mesangial cells. A) ROS, superoxide was measured by DHE fluorescent activity as described in the material and methods. B) Quantification of DHE fluorescence measured by image j software. Values are the mean ± SEM; $n = 8$; $^{*}p < .05$ versus control; $^{\#,\dagger}p < .05$ versus Hcy treated cells.

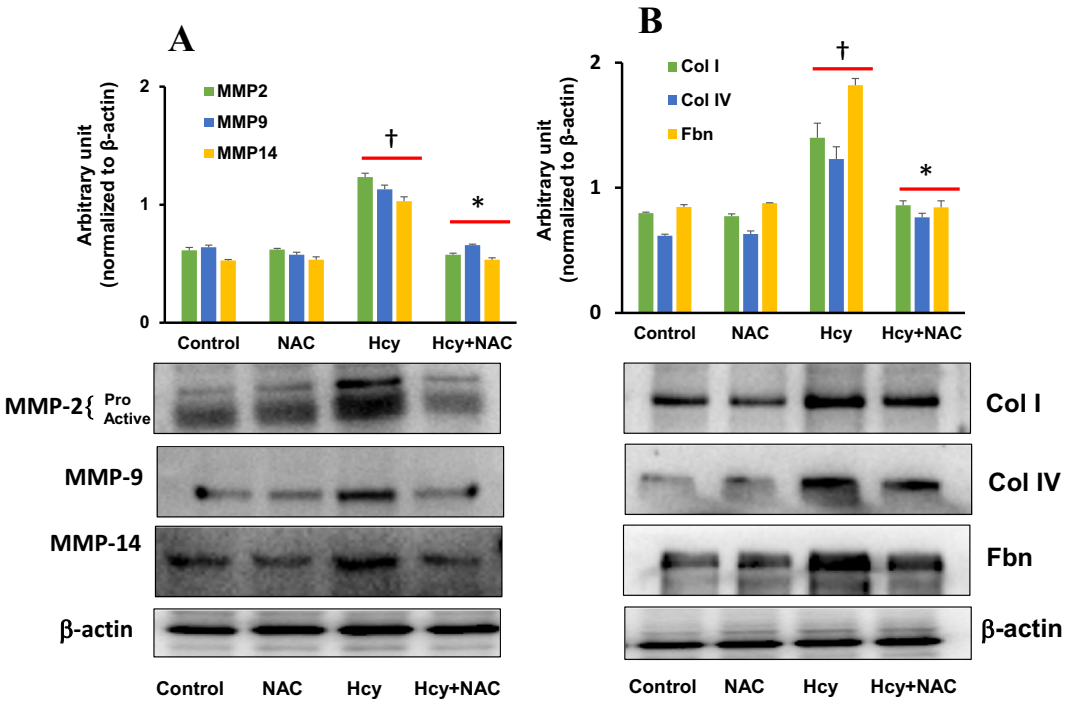

Fig. 8. Hcy-induced altered expression of MMP-2, -9, -14 and Col I, Col IV, Fibronectin (Fbn) was normalized by NAC treatment. (A) The protein expression of MMP-2, -9, -14 and Col I, Col IV, Fbn in mesangial cells treated with Hcy with or without NAC was measured by Western blotting. (B) Bar graphs represent the quantitative measurement of protein expression normalized with β-actin. Values are mean ± SEM, $n = 9$ independent experiments; $^{\dagger}p < .05$ vs. Control, and $^{*}p < .05$ vs. Hcy alone.

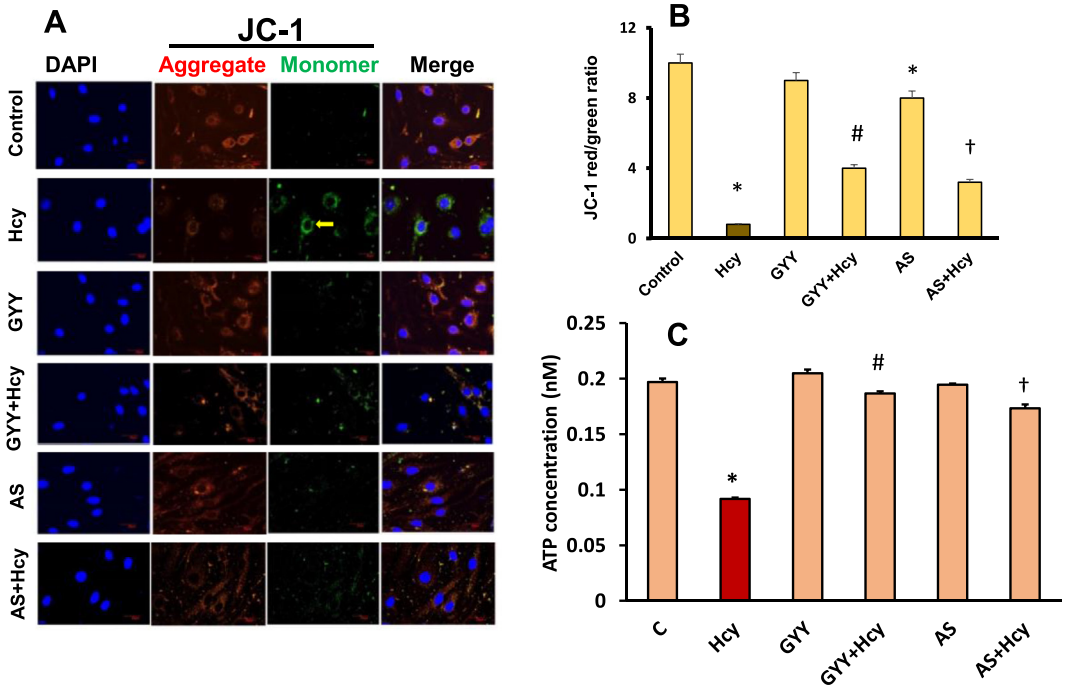

Fig. 9. GYY4137 (GYY) and AS1842856 (AS) treatment reduced Hcy-induced mitochondrial depolarization and increased intercellular ATP concentration. A) Fluorescence microscopic images of cells subjected to JC-1 staining (60×), scale bar 50 μm. Cells were exposed to Hcy (50 μM) for 24 h with or without GYY and AS. Red staining indicates polarized mitochondria in control, GYY and AS treated cells; green staining indicates depolarized mitochondria in Hcy treated cells. B) The bar diagram represents the quantification of JC-1 red-to-green ratio. Values are the mean ± SEM; $n = 8$ independent experiments. $^{*}p < .05$ versus control; $^{\#,\dagger}p < .05$ versus Hcy treatment. C) Hcy induced reduction of intracellular ATP concentration was restored by GYY and AS treatment. Values are the mean ± SEM; $n = 9$ independent experiments. $^{*}p < .05$ versus control; $^{\#,\dagger}p < .05$ versus Hcy treated cells. (For interpretation of the references to colour in this figure legend, the reader is referred to the web version of this article.)

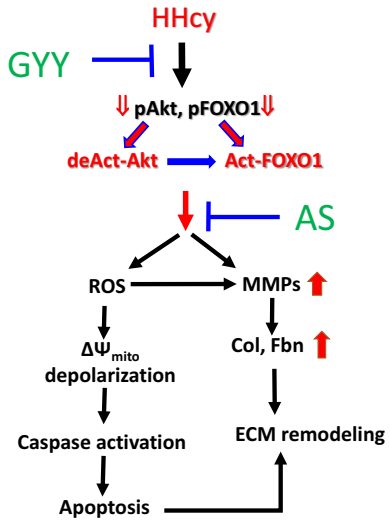

Fig. 10. Schematic of overall findings. Hcy dephosphorylates both Akt and FOXO1 causing Akt deactivation and FOXO1 activation. These leads to ROS-mediated cellular apoptosis, MMPs activation, and fibronectin and collagen deposition. GYY and AS prevents apoptosis and Fbn and collagen deposition, and thus ECM remodelling otherwise induced by Hcy. resulting in ECM and fibronectin induction leading to ECM remodelling. GYY and AS Inhibition of$\Delta\Psi$ mito depolarization, mitochondrial membrane depolarization. pAkt, phospho-Akt; deAct-Akt, deactivated Akt; pFOXO1, phospho-FOXO1; Act-FOXO1, Activated FOXO1.

kidney dysfunction. Previously our laboratory has established that H_2S supplementation is an effective treatment strategy to protect the kidney from HHcy associated malfunctioning [6,7]. Recent findings from our laboratory also demonstrated that GYY4137 (GYY), a H_2S donor alleviated hypertensive kidney dysfunction and collagen realignment in the diabetic kidney [24,33]. Studies from other laboratories have further confirmed that GYY ameliorates cardiac and other vascular damages [31,34]. Until now and to our best knowledge, no report is available suggesting specific signalling mechanism of the protective effect of GYY in HHcy-associated cellular damage in the kidney. Our present report bridges this knowledge gap and highlights the important signalling mechanism suggesting the protective role of GYY on mouse mesangial cells in HHcy. In Fig. 10, we schematically present our findings from this study for easy comprehension.

Results from the present study demonstrate that Hcy inhibited Akt activation and promoted FOXO1 activation by diminishing phosphorylation of both these signalling molecules. Deactivation and activation of Akt and FOXO1, respectively caused by dephosphorylation of these signalling molecules that led to cellular apoptosis and upregulation of MMP-2, -9, -14 gene and protein expression contributing to increased ECM protein synthesis including collagen and fibrinogen, causing mesangial ECM remodelling. We also provided evidence that Hcy-induced mesangial cell apoptosis was associated with excess ROS production, mitochondrial membrane depolarization, and caspase activation. These detrimental changes in HHcy were mitigated either by GYY or AS treatment that modulated Akt/FOXO1 signalling axis, where Akt appeared to be the upstream signalling of FOXO1. In Fig. 10, we proposed the most possible mechanistic model based on our overall findings depicting how GYY and/or AS protects mesangial cells from apoptotic remodelling by regulating Akt/FOXO1 signalling pathway in HHcy condition.

Previous report suggests an interaction between membrane type-1 matrix metalloproteinase (MT1-MMP; MMP-14) and Akt kinase that induced endothelial cellular apoptosis [35]. Similarly, FOXO1 is also reported to be involved in promoting apoptosis in mitochondria-dependent and - independent manner [36]. In addition, reports are available that the axis of Akt/FOXO1 regulated a number of cellular events including hepatic regeneration [37], osteoblast differentiation [38], cellular proliferation and cell death [39], and cardiac tissue remodelling [40]. Although, Akt/FOXO1-dependent regulation of H_2S generation has been reported in endothelial dysfunction in portal hypertension [41], the reverse mechanism, i.e. whether H_2S regulates Akt/FOXO1 is not well known. In our first set of experiments, we detected significantly lower level of pAkt and pFOXO1 protein expression in Hcy treated mesangial cells, which was reversed by H_2S donor, GYY. GYY activated Akt, a cell survival factor, which further downregulated FOXO1 activation and protected cells from Hcy threat (Fig. 1). This result further supports the previous finding that FOXO1 is downstream of Akt signalling [15], and that Akt/FOXO1 is involved in cellular apoptosis in HHcy.

Extracellular matrix (ECM) turnover is one of the major pathological factors contributing to HHcy-associated renal fibrosis that leads to a progressive decline of renal function in CKD [31,32]. Previously our laboratory showed that ROS plays an important role in Hcy-induced ECM remodelling in glomerulus by regulating the MMPs activity and collagen deposition [7]. Both ECM synthesis and degradation are maintained by MMPs, and changes in MMPs expression and activity can lead to ECM accumulation. In the present study, we detected Hcy-mediated significant increase in MMP-2, -9, and -14 mRNA and protein expression in mesangial cells, which were normalized by GYY treatment (Fig. 2). FOXO1 inhibitor, AS treatment, also diminished Hcy-mediated overexpression of MMP-2, -9 and -14. We also observed Hcy induced collagen I (Col 1), collagen IV (Col IV) and fibronectin-1 (Fbn-1) protein expression in mesangial cells, which was normalized by GYY treatment (Fig. 3). FOXO1 inhibition also normalized Hcy-induced overexpression of Col I, Col IV and Fbn-1 in mesangial cells (Figs. 3, 4). These results reveal that GYY or AS treatment mitigates excess ECM synthesis and accumulation in mesangial cells by modulating Akt/FOXO1 signalling cascade in HHcy. It is noteworthy to mention that we detected MMP-14, Col IV and Fbn1 expression in mesangial cells by immunofluorescence (Fig. 4). The results indicated that they are localized mostly to the cytoplasm. We did not measure whether they are secreted into the extracellular fluid/culture medium. This important question of cellular biology remained unanswered in our study, which may occur in response to Hcy stress. Only future study can reveal whether Hcy-induction leads to ECM protein secretion from mesangial cells into the extracellular fluid and whether GYY or AS can modulate their section, if any in HHcy.

Recently, Hcy has been reported to induce endothelial cell apoptosis by modulating the mitochondrial-dependent Akt pathway [42]. In addition, H_2S has also been shown to reduce Hcy-induced neuronal cell death [43]. In our present study, we observed that Hcy promoted mesangial cell apoptosis, which was mitigated by treatment with H_2S donor, GYY (Fig. 5). To further verify whether the Hcy effect was through Akt, we treated cells with Akt inhibitor MK2206 (MK) with or without Hcy. Our results indicated that increasing number of cellular apoptosis was measured in cells treated with Hcy plus MK, compared to Hcy or MK alone (Fig. 5). These results confirmed that Hcy induced Akt inactivation led mesangial cell death. On the other hand, this result was in contrast to healthy cells, where Akt inhibited FOXO1 activation and protected cells from apoptosis. To verify the involvement of FOXO1, we treated cells with FOXO1 inhibitor AS, and results indicated significant attenuation of Hcy-induced cellular apoptosis (Fig. 5). These results suggest a probable regulatory role of Akt/FOXO1 signalling in GYY-mediated recovery of cellular damage in HHcy conditions.

Studies have reported that apoptotic cell death in renal mesangial cells occurred due to enhanced mitochondrial oxidative stress leading to mitochondrial membrane depolarization and followed by caspase activities [44,45]. The association between excessive production of intracellular reactive oxygen species (ROS) and Hcy-induced renal damage is already been an established fact [7,21]. However, the connection between caspase and oxidative stress in Hcy-induced mesangial

cell death is not clear in the literature. Our results demonstrated Hcy induced caspase-3/7 expression and ROS production in mesangial cells (Figs. 6 and 7, respectively). Further studies revealed that treatment with a H_2S donor, GYY or FOXO1 inhibitor, AS diminished caspase-3/7 overexpression and reduced ROS production in mesangial cells. These findings suggest the involvement and the regulation of FOXO1 pathway by H_2S, which mitigates Hcy-induced oxidative stress and caspase activation, and thus diminishes cellular apoptosis.

We and others have shown that Hcy induces oxidative stress, which in turn induces MMPs in a variety of pathological conditions, both in vivo and in vitro settings [32,46,47]. Changes in MMPs expression and activity can lead to disproportional ECM synthesis and accumulation causing deleterious vascular remodelling [48,49]. Normal human kidney expresses MMP-2 and -9 at a very low level [50], however during progressive renal fibrosis, the mRNA transcription and protein expression of MMP-2 and -9 were shown to be upregulated in human and rodent's kidney [51–53]. In addition, overexpressed MMP-14 mRNA was also reported predominantly in cyst-lining epithelia in experimental polycystic kidney disease, and MMP inhibitor therapy decreased cyst formation [54]. It is important to mention that MMP-2 and -9 are collagenases, and studies have shown the renoprotective effects of these MMPs through promoting matrix turnover and thus preventing ECM accumulation [55,56]. On the contrary, elevated expressions and activities of MMP-2 and -9 have been observed in the fibrotic renal cortex suggesting their role in matrix accumulation associated with progressive renal scarring [57]. The mechanism of these paradoxical roles of MMPs is mostly unexplained in the literature. A possible explanation is that, in addition to collagen degradation, MMP-2 and -9 also degrade elastin [58]. And because the turnover of collagen is faster than elastin [59], oxidatively modified collagen is deposited faster than elastin or any other ultra-structural matrix proteins in an increased oxidant environment [29]. This causes ECM accumulation in certain disease conditions, such as in HHcy, where MMPs expression and activity are upregulated favouring fibrosis development.

To determine whether Hcy-induced oxidative stress causes MMP-2, -9 and -14 dysregulation and ECM protein overexpression, and whether scavenging ROS by NAC in HHcy normalizes these MMPs expression and thus ECM protein, we threated mesangial cells with or without NAC along with Hcy. Our results indicated that Hcy mediated a significant increase of MMP-2, -9, and -14 protein expression in mesangial cells, which was normalized by NAC treatment (Fig. 8). We also observed Hcy-induced collagen I (Col 1), collagen IV (Col IV) and fibronectin-1 (Fbn-1) protein overexpression in mesangial cells was normalized by NAC treatment (Fig. 8). These results suggest that Hcy-induces ROS and prevention of ROS production by NAC mitigates MMPs and ECM protein overexpression in mesangial cells. These findings are also in corroboration with our results that GYY mitigates MMPs and ECM protein expression through reducing ROS production (Figs. 2–4, and 7, respectively).

Several studies have shown mitochondrial membrane depolarization is directly linked to excess ROS associated cellular damage [38]. To investigate the direct effect of Hcy-mediated ROS production in mesangial cells, we measured mitochondrial membrane potential ($\Delta\Psi m$) and intracellular ATP concentration. The membrane-permeant JC-1 dye has widely been used as an indicator of $\Delta\Psi m$. The dye exhibits potential-dependent accumulation in mitochondria, which is indicative of a shift of fluorescence emission from green to red. Thus, a decrease in the red/green fluorescence intensity ratio indicates mitochondrial depolarization. Our results indicated Hcy treatment caused a loss of mitochondrial membrane polarization as well as reduced ATP concentration in mesangial cells (Fig. 9), suggesting mitochondrial depolarization and ATP reduction. Interestingly, GYY treatment prevented depolarization and reserved ATP concentration. Similarly, FOXO1 inhibitor AS also prevented Hcy-induced loss of $\Delta\Psi m$ and reserved ATP concentration (Fig. 9). These results suggest that Hcy-induced loss of $\Delta\psi m$ was through the reduction of H_2S and FOXO1 pathway.

In conclusion, our study demonstrates that H_2S donor, GYY mitigates HHcy associated mesangial cell death by attenuating excessive ROS production, ameliorating the loss of mitochondrial membrane potential ($\Delta\Psi m$), preserving intracellular ATP concentration and by reducing caspase activation, which otherwise lead to collagen and fibrinogen synthesis resulting in cellular apoptosis and ECM remodelling. We also provide evidence that these effects of Hcy were mediated via Akt/FOXO1 signalling pathway, and that H_2S mitigates Akt/FOXO1 cascade to exert its protective effect in HHcy condition.

Acknowledgments

We thank Aron Tyagi for technical assistance in maintaining cell culture and setting up for experiments.

Grants

This work was supported in part by National Institutes of Health Grants, DK104653 and DK116591 (to U.S.), and American Heart Association Scientist Development Grant, 15SDG25840013 (to S.P.)

Disclosures

The authors declare no conflicts of interest, financial or otherwise.

Authors contributions

SM, LR and US conceived the idea and designed experiments; SM and LR performed experiment, analyzed the data and interpreted the results, prepared figures and drafted the manuscript; SP contributed to experiments; SM and US edited, revised and approved final version of the manuscript.

References

[1] J. Yang, P. Fang, D. Yu, L. Zhang, D. Zhang, X. Jiang, W.Y. Yang, T. Bottiglieri, S.P. Kunapuli, J. Yu, E.T. Choi, Y. Ji, X. Yang, H. Wang, Circ. Res. 119 (2016) 1226–1241.
[2] K. Nagai, T. Tominaga, S. Ueda, E. Shibata, M. Tamaki, M. Matsuura, S. Kishi, T. Murakami, T. Moriya, H. Abe, T. Doi, J. Am. Soc. Nephrol. 28 (2017) 2879–2885.
[3] V. Klemis, H. Ghura, G. Federico, C. Wurfel, A. Bentmann, N. Gretz, T. Miyazaki, H.J. Grone, I.A. Nakchbandi, Kidney Int. 91 (2017) 1374–1385.
[4] L.L. Liu, L.B. Zhu, J.N. Zheng, T.D. Bi, J.F. Ma, L.N. Wang, L. Yao, Sci. Rep. 8 (2018) 7309.
[5] X. Zhang, S. Shi, Y. Ouyang, M. Yang, M. Shi, X. Pan, J. Lv, Z. Wang, H. Ren, P. Shen, W. Wang, H. Zhang, J. Xie, N. Chen, J. Transl. Med. 16 (2018) 115.
[6] U. Sen, C. Munjal, N. Qipshidze, O. Abe, R. Gargoum, S.C. Tyagi, Am. J. Nephrol. 31 (2010) 442–455.
[7] U. Sen, P. Basu, O.A. Abe, S. Givvimani, N. Tyagi, N. Metreveli, K.S. Shah, J.C. Passmore, S.C. Tyagi, Am. J. Physiol. Ren. Physiol. 297 (2009) F410–F419.
[8] Y. Fan, W. Xiao, Z. Li, X. Li, P.Y. Chuang, B. Jim, W. Zhang, C. Wei, N. Wang, W. Jia, H. Xiong, K. Lee, J.C. He, Nat. Commun. 6 (2015) 7841.
[9] J. Jin, L. Jin, S.W. Lim, C.W. Yang, Am. J. Nephrol. 43 (2016) 357–365.
[10] K.W. Joo, S. Kim, S.Y. Ahn, H.J. Chin, D.W. Chae, J. Lee, J.S. Han, K.Y. Na, BMC Nephrol. 14 (2013) 98.
[11] F. Li, L. Li, M. Cheng, X. Wang, J. Hao, S. Liu, H. Duan, Biochem. Biophys. Res. Commun. 482 (2017) 1477–1483.
[12] D. Zhang, J. Pan, X. Xiang, Y. Liu, G. Dong, M.J. Livingston, J.K. Chen, X.M. Yin, Z. Dong, J. Am. Soc. Nephrol. 28 (2017) 1131–1144.
[13] Y. Wang, Y. Zhou, D.T. Graves, Biomed. Res. Int. 2014 (2014) 925350.
[14] M. Farhan, H. Wang, U. Gaur, P.J. Little, J. Xu, W. Zheng, Int. J. Biol. Sci. 13 (2017) 815–827.
[15] X. Zhang, N. Tang, T.J. Hadden, A.K. Rishi, Biochim. Biophys. Acta 1813 (2011) 1978–1986.
[16] X. Wang, C. Lin, X. Zhao, A. Liu, J. Zhu, X. Li, L. Song, Mol. Cancer 13 (2014) 106.
[17] M. Fang, A. Jin, Y. Zhao, X. Liu, Braz. J. Med. Biol. Res. 49 (2016) e4543.
[18] R.F. Huang, S.M. Huang, B.S. Lin, C.Y. Hung, H.T. Lu, J. Nutr. 132 (2002) 2151–2156.
[19] X. Tian, Y. Shi, N. Liu, Y. Yan, T. Li, P. Hua, B. Liu, Mol. Med. Rep. 14 (2016) 4173–4179.
[20] Z. Zhang, C. Wei, Y. Zhou, T. Yan, Z. Wang, W. Li, L. Zhao, Oxidative Med. Cell. Longev. 2017 (2017) 5736506.
[21] S. Shastry, A.J. Ingram, J.W. Scholey, L.R. James, Kidney Int. 71 (2007) 304–311.
[22] H.S. Zhang, E.H. Cao, J.F. Qin, Pharmacology 74 (2005) 57–64.

[23] S. Kundu, S.B. Pushpakumar, A. Tyagi, D. Coley, U. Sen, Am. J. Physiol. Endocrinol. Metab. 304 (2013) E1365–E1378.
[24] A. John, S. Kundu, S. Pushpakumar, M. Fordham, G. Weber, M. Mukhopadhyay, U. Sen, Sci. Rep. 7 (2017) 10924.
[25] S. Lin, D. Lian, W. Liu, A. Haig, I. Lobb, A. Hijazi, H. Razvi, J. Burton, M. Whiteman, A. Sener, Nitric Oxide Biol. Chem. 76 (2018) 16–28.
[26] S. Lilyanna, M.T. Peh, O.W. Liew, P. Wang, P.K. Moore, A.M. Richards, E.C. Martinez, J. Mol. Cell. Cardiol. 87 (2015) 27–37.
[27] J.D. Ly, D.R. Grubb, A. Lawen, Apoptosis 8 (2003) 115–128.
[28] G. Berg, M. Barchuk, V. Miksztowicz, Cells 8 (2019).
[29] T.M. Camp, S.C. Tyagi, R.M. Senior, M.R. Hayden, S.C. Tyagi, Diabetologia 46 (2003) 1438–1445.
[30] C. van Guldener, Nephrol. Dial. Transplant. 21 (2006) 1161–1166.
[31] S. Li, B. Qiu, H. Lu, Y. Lai, J. Liu, J. Luo, F. Zhu, Z. Hu, M. Zhou, J. Tian, Z. Zhou, S. Yu, F. Yi, J. Nie, Antioxid. Redox Signal. 30 (13) (2019) 1635–1650.
[32] S.B. Pushpakumar, S. Kundu, N. Metreveli, U. Sen, PLoS One 8 (2013) e83813.
[33] G.J. Weber, S.B. Pushpakumar, U. Sen, Am. J. Physiol. Heart Circ. Physiol. 312 (2017) H874–H885.
[34] B. Tang, L. Ma, X. Yao, G. Tan, P. Han, T. Yu, B. Liu, X. Sun, J. Vasc. Surg. 65 (2017) 501–508 (e501).
[35] H. Ohkawara, T. Ishibashi, K. Sugimoto, K. Ikeda, K. Ogawa, Y. Takeishi, PLoS One 9 (2014) e105697.
[36] Z. Fu, D.J. Tindall, Oncogene 27 (2008) 2312–2319.
[37] M. Pauta, N. Rotllan, A. Fernandez-Hernando, C. Langhi, J. Ribera, M. Lu, L. Boix, J. Bruix, W. Jimenez, Y. Suarez, D.A. Ford, A. Baldan, M.J. Birnbaum, M. Morales-Ruiz, C. Fernandez-Hernando, Hepatology 63 (2016) 1660–1674.
[38] T. Moriishi, Y. Kawai, H. Komori, S. Rokutanda, Y. Eguchi, Y. Tsujimoto, I. Asahina, T. Komori, PLoS One 9 (2014) e86629.
[39] R. Karki, R.K.S. Malireddi, Q. Zhu, T.D. Kanneganti, Cell Cycle 16 (2017) 1243–1251.
[40] W.B. Zhang, Q.J. Du, H. Li, A.J. Sun, Z.H. Qiu, C.N. Wu, G. Zhao, H. Gong, K. Hu, Y.Z. Zou, J.B. Ge, J. Cell. Mol. Med. 16 (2012) 2227–2237.
[41] B. Renga, S. Cipriani, A. Carino, M. Simonetti, A. Zampella, S. Fiorucci, PLoS One 10 (2015) e0141082.
[42] S. Liu, Z. Sun, P. Chu, H. Li, A. Ahsan, Z. Zhou, Z. Zhang, B. Sun, J. Wu, Y. Xi, G. Han, Y. Lin, J. Peng, Z. Tang, Apoptosis 22 (2017) 672–680.
[43] H.J. Wei, J.H. Xu, M.H. Li, J.P. Tang, W. Zou, P. Zhang, L. Wang, C.Y. Wang, X.Q. Tang, Acta Pharmacol. Sin. 35 (2014) 707–715.
[44] L. Xu, Q. Fan, X. Wang, X. Zhao, L. Wang, Cell Death Dis. 7 (2016) e2445.
[45] D. Wu, X. Chen, D. Guo, Q. Hong, B. Fu, R. Ding, L. Yu, K. Hou, Z. Feng, X. Zhang, J. Wang, J. Am. Soc. Nephrol. 16 (2005) 646–657.
[46] L.J. Winchester, S. Veeranki, S. Pushpakumar, S.C. Tyagi, Phys. Rep. 6 (2018) e13637.
[47] X.D. Ke, A. Foucault-Bertaud, C. Genovesio, F. Dignat-George, E. Lamy, P. Charpiot, Mol. Cell. Biochem. 335 (2010) 203–210.
[48] I. Wiernicki, M. Parafiniuk, A. Kolasa-Wolosiuk, I. Gutowska, A. Kazimierczak, J. Clark, I. Baranowska-Bosiacka, P. Szumilowicz, P. Gutowski, FASEB J. 33 (1) (2019) 885–895 fj201800633R.
[49] V.A. Myasoedova, D.A. Chistiakov, A.V. Grechko, A.N. Orekhov, J. Mol. Cell. Cardiol. 123 (2018) 159–167.
[50] Z. Cheng, M.H. Limbu, Z. Wang, J. Liu, L. Liu, X. Zhang, P. Chen, B. Liu, Int. J. Mol. Sci. 18 (2017).
[51] J.P. Tsai, J.H. Liou, W.T. Kao, S.C. Wang, J.D. Lian, H.R. Chang, PLoS One 7 (2012) e48164.
[52] C. Ruster, G. Wolf, Am. Soc. Nephrol. 22 (2011) 1189–1199.
[53] D. Cosgrove, B. Dufek, D.T. Meehan, D. Delimont, M. Hartnett, G. Samuelson, M.A. Gratton, G. Phillips, D.A. MacKenna, G. Bain, Kidney Int. 94 (2018) 303–314.
[54] N. Obermuller, N. Morente, B. Kranzlin, N. Gretz, R. Witzgall, Am. J. Physiol. Ren. Physiol. 280 (2001) F540–F550.
[55] T. Endo, K. Nakabayashi, M. Sekiuchi, T. Kuroda, A. Soejima, A. Yamada, Clin. Exp. Nephrol. 10 (2006) 253–261.
[56] J. Rysz, M. Banach, R.A. Stolarek, J. Pasnik, A. Cialkowska-Rysz, R. Koktysz, M. Piechota, Z. Baj, J. Nephrol. 20 (2007) 444–452.
[57] V.H. Rao, G.E. Lees, C.E. Kashtan, R. Nemori, R.K. Singh, D.T. Meehan, K. Rodgers, B.R. Berridge, G. Bhattacharya, D. Cosgrove, Kidney Int. 63 (2003) 1736–1748.
[58] R.M. Senior, G.L. Griffin, C.J. Fliszar, S.D. Shapiro, G.I. Goldberg, H.G. Welgus, J. Biol. Chem. 266 (1991) 7870–7875.
[59] D.J. Johnson, J. LaBourene, M. Rabinovitch, F.W. Keeley, Connect. Tissue Res. 29 (1993) 213–221.
[60] S. Pushpakumar, L. Ren, S. Kundu, A. Gamon, S.C. Tyagi, U. Sen, Sci. Rep. 7 (2017) 6349.